四川大学学报（医学版） 2024，55（6）：1403－1409
J Sichuan Univ（Med Sci）

在线全文

深度学习重建算法联合智能去除金属伪影技术改善危重患者上腹部CT的图像质量*

潘云龙， 姚小玲， 高荣慧， 谢 薇， 夏春潮， 李真林， 孙怀强△
四川大学华西医院 放射科 华西磁共振研究中心（成都 610041）

【摘要】 目的 评估基于深度学习算法联合智能去除金属伪影技术（deep learning combined with smart metal artifact reduction, DLMAR）对无法举起手臂且需要心电监护的危重患者上腹部CT图像质量的影响。**方法** 回顾性纳入无法举起手臂且需要心电监护的102例危重患者。对图像静脉期分别采用滤波反投影（filtered back projection, FBP）、迭代重建（iterative reconstruction, IR）、深度学习（deep learning, DL）、滤波反投影联合智能去除金属伪影技术（filtered back projection combined with smart metal artifact reduction, FBPMAR）、自适应统计迭代重建联合智能去除金属伪影技术（adaptive statistical iterative reconstruction-V combined with smart metal artifact reduction, IRMAR）、DLMAR共6种算法重建图像。对肝脏无伪影区域、肝脏有金属伪影区域、两手臂间组织（肝、脾、胰、主动脉）的CT值、噪声、信噪比（signal-to-noise ratio, SNR）、对比度噪声比（contrast-to-noise ratio, CNR）进行定量分析。并采用5级评分法，对电极金属伪影、两手臂间结构的显示和图像噪声进行定性分析（1=最差，5=最佳）。**结果** 在肝脏有金属伪影的区域：DLMAR组〔（98.5±9.8）HU〕与FBP组〔（73.7±5.6）HU〕、IR组〔（75.3±7.5）HU〕、DL组〔（66.3±11.4）HU〕的CT值差异有统计学意义（P<0.01）；DLMAR与FBPMAR〔（99.8±4.8）HU〕、IRMAR〔（99.6±3.4）HU〕的CT值差异无统计学意义；DLMAR噪声均低于其他组（P<0.01）；DLMAR的SNR和CNR均高于其他组（P<0.01）。在两手臂间组织区域：6组的CT值差异无统计学意义；DLMAR噪声均低于其他组（P<0.01）；DLMAR的SNR和CNR均高于其他组（P<0.01）。FBPMAR、IRMAR、DLMAR组在去金属伪影方面的得分（4.27±0.32、4.44±0.34、4.61±0.28）均高于FBP、IR、DL组（1.36±0.54、1.32±0.45、1.24±0.46）（P<0.01）。DLMAR组在两手臂间结构显示得分4.62±0.37，图像降噪得分4.53±0.39，均高于其他组（P<0.01）。**结论** 在双手臂不能上举，且需要心电监护的危重患者中，DLMAR可以减少伪影、降低噪声，提升上腹部CT图像质量。

【关键词】 深度学习 金属伪影 危重患者 腹部计算机断层扫描

Deep Learning Reconstruction Algorithm Combined With Smart Metal Artifact Reduction Technique Improves Image Quality of Upper Abdominal CT in Critically Ill Patients

PAN Yunlong, *YAO Xiaoling*, *GAO Ronghui*, *XIE Wei*, *XIA Chunchao*, *LI Zhenlin*, *SUN Huaiqiang*△. *Huaxi MR Research Center* (*HMRRC*), *Department of Radiology*, *West China Hospital*, *Sichuan University*, Chengdu 610041, China
△ Corresponding author, E-mail: sunhuaiqiang@scu.edu.cn

【Abstract】 Objective To evaluate the effect of deep learning reconstruction algorithm combined with smart metal artifact reduction (DLMAR) on the quality of abdominal CT images in critically ill patients who are unable to raise their arms and require electrocardiographic (ECG) monitoring. **Methods** A total of 102 patients were retrospectively enrolled. All subjects were critically ill patients who were unable to raise their arms and required ECG monitoring. Images were reconstructed using 6 algorithms, including filtered back projection (FBP), iterative reconstruction (IR), deep learning (DL), FBP combined with smart metal artifact reduction (FBPMAR), adaptive statistical iterative reconstruction-V combined with smart metal artifact reduction (IRMAR), and DLMAR. A quantitative analysis of CT values, noise, signal-to-noise ratio (SNR), and contrast-to-noise ratio (CNR) was conducted in regions without metal artifacts and regions with metal artifacts in the liver, as well as the tissues, including those from the liver, spleen, pancreas, and aorta, between the two arms. Qualitative analysis of electrode metal artifacts, the visualization of the structures between the two arms, and image noise was performed with a 5-point scoring system (1=worst and 5=best). **Results** In the regions of the liver with metal artifacts, there was a significant difference between the CT values of the DLMAR group ([98.5±9.8] Hounsfield units [HU]) and those of the FBP group ([73.7±5.6] HU), the IR group ([75.3±7.5] HU), and the DL group ([66.3±11.4] HU) (P<0.01). There was no significant difference between the CT values of the DLMAR group and those of the FBPMAR group ([99.8±4.8] HU) and the IRMAR group ([99.6±3.4] HU) (P>0.05). The noise of the DLMAR group was found to be significantly lower than that of the other groups (P<0.01). Furthermore, the SNR and CNR of the DLMAR group were also found to be higher than those of the other groups (P<0.01). In the tissue region between the two

* 四川省科技厅重点研发项目（No. 2023YFG0126）和四川大学华西医院学科卓越发展1·3·5工程项目（No. ZYGD23024）资助
△ 通信作者，E-mail: sunhuaiqiang@scu.edu.cn
出版日期：2024-11-20

arms, the differences in CT values among the six groups were not statistically significant (P>0.05). The noise of the DLMAR group was lower than those of the other groups (P<0.01), and the SNR and CNR of the DLMAR group were higher than those of the other groups (P<0.01). In terms of the removal of metal artifacts, the scores of the FBPMAR, IRMAR, and DLMAR groups (4.27±0.32, 4.44±0.34, and 4.61±0.28, respectively) were higher than those of the FBP, IR, and DL groups (1.36±0.54, 1.32±0.45, and 1.24±0.46, respectively) (P<0.01). The DLMAR group also had a higher score of 4.62±0.37 in the visualization of structures between the two arms and 4.53±0.39 in the noise reduction of images, both of which were higher than those of the other groups (P<0.01). **Conclusion** DLMAR reduces artifacts, decreases noise, and improves the quality of abdominal CT imaging in critically ill patients who are unable to raise their arms and require ECG monitoring.

【Key words】 Deep learning Metal artifact Critically ill patients Abdominal CT

危重患者的病情常多变且危急。CT扫描速度快，禁忌证少和能提供详尽的解剖结构及病变信息等能力，已成为评估危重患者的常规检查方法[1-4]。部分危重患者由于肩部或手臂外伤以及意识障碍等原因无法上举双手且需要携带心电监护。人为地举起手臂和去除心电监护，这类危重患者则易发生安全事故[5]。在这类危重患者进行CT腹部扫描时，两手臂间的图像噪声大、条纹伪影重[6]，心电监护的电极片和电极线将产生金属伪影[7]。

YASAKA等[8]研究表明对于双手臂不能上举的患者，迭代重建(iterative reconstruction, IR)可减少双手臂间的条纹伪影。但IR重建时间长，重建图像纹理可能存在蜡像感，易产生边缘清晰度伪影[9-11]。深度学习(deep learning, DL)重建能降低噪声，提高信噪比且无重建伪影[12]；智能去除金属伪影技术(smart metal artifact reduction, smart MAR)能解决金属伪影问题[13]。深度学习算法联合智能去除金属伪影技术(deep learning combined with smart metal artifact reduction, DLMAR)可结合DL和smart MAR技术的优点，降低噪声，减少金属伪影，提高信噪比，将这项新技术应用在特殊患者检查中，可解决这类患者目前存在的临床问题。

目前针对这类危重患者的CT图像重建研究较少，多为迭代算法，且没有解决金属伪影的问题。本研究在常规检查辐射剂量下，通过对比滤波反投影(filtered back projection, FBP)、IR、DL、滤波反投影联合智能去除金属伪影技术(perform filtered back projection combined with smart metal artifact reduction, FBPMAR)、自适应统计迭代重建联合智能去除金属伪影技术(adaptive statistical iterative reconstruction-V combined with smart metal artifact reduction, IRMAR)、DLMAR共6组重建图像，探讨DLMAR是否可以减少这类危重患者CT图像伪影，提高上腹部图像质量。上腹部平扫、动脉期和静脉期成像参数及伪影产生原因基本一致，本研究选择静脉期进行分析。

1 资料与方法

1.1 研究人群

本研究回顾性纳入2023年2–12月在四川大学华西医院接受CT检查的危重患者。患者纳入标准：①双手不能上举；②带有心电监护仪(图1)；③检查项目包含上腹部CT增强。排除标准：①图像强化效果差；②呼吸运动伪影明显；③原始数据缺失。本研究经四川大学华西医院伦理委员会批准(2019年审206号)，免征每例患者的知情同意书。在分析之前，患者信息和重建方法已被匿名化。

图 1 危重患者扫描胸及上腹的定位像

Fig 1 Localized image of a critically ill patient's CT scan of the chest and upper abdomen

1.2 CT图像采集参数

所有患者均在256排CT扫描仪(Revolution Apex CT, GE Healthcare)上接受检查。腹部扫描参数如下：管电压120 kV，管电流采用自动调制技术，自动调制范围为250 ~ 500 mA，噪声指数为8.5，螺距0.992∶1，球管旋转时间为0.5 s，探测器宽度为80 mm。采用高压注射器通过肘静脉注射对比剂(碘佛醇320 mgI/mL，中国江苏恒瑞医药股份有限公司)，注射速度为2.5 mL/s，注射量根据体质量计算(体质量×1.5 mL/kg，最高不超过100 mL)。在门静脉层面的降主动脉设置Bolus跟踪，并在达到120 HU的阈值后5.9 s屏气采集动脉期，静脉期扫描时间为触发后45 ~ 55 s。

1.3　图像重建

本研究采用GE公司的深度学习图像重建算法, 该算法经过高质量FBP数据集的训练, 学习如何区分噪声和信号, 并在不影响解剖和病理结构的情况下智能抑制噪声, 生成高质量的CT图像。

本研究采用GE公司的Smart MAR技术, 该技术采用了自动化、三阶段的基于投影的处理过程, 旨在提高CT数据的质量。首先, 通过识别在投影中对应于金属物体的受损样本, 确定受金属干扰的区域。其次, 通过用已校正的数据替代这些受金属干扰的投影, 生成修复后的数据。这一校正过程借助对分类图像的正向投影来实现。最后, 通过将原始投影数据与修复后的投影数据进行组合, 生成了最终的校正投影, 揭示伪影下隐藏的解剖细节。

在本机保存的原始数据上, 对静脉期CT上腹部分别采用FBP、IR、DL、FBPMAR、IRMAR、DLMAR重建图像。其中涉及的IR采用自适应统计迭代重建(adaptive statistical iterative reconstruction-V, ASIR-V)50%, 涉及的DL采用中等强度。重建层厚/层间距2.5 mm/2.5 mm。将所有重建图像上传到后处理工作站adw4.7。

1.4　图像质量评价

1.4.1　定量图像质量评价

为定量分析手臂和金属电极对上腹部组织衰减的影响, 由一名高年资医师(6年腹部诊断经验)勾画感兴趣区域(region of interest, ROI)进行定量测量。ROI定义为以下区域: ROI1, 肝脏无金属伪影区域, 选择肝脏左外叶中间层面无伪影区域; ROI2, 肝脏有金属伪影区域, 选择肝脏层面金属伪影重区域; ROI3, 两手臂间脾脏区域; ROI4, 两手臂间肝脏区域; ROI5, 两手臂间腹主动脉区域; ROI6, 两手臂间胰腺区域; ROI7, 腹部皮下无伪影脂肪区域(图2)。将每例患者的6组重建图像设置并排同时显示, 并在z轴方向上匹配, 每个ROI在 FBP组图像中定义, 然后复制到其他组的同一层面, 记录ROI平均 CT值和相应的标准差(standard deviation, SD)。ROI的大小、形状尽可能保持一致, 避免钙化灶及相邻组织。采用HU/SD计算信噪比(signal-to-noise ratio, SNR), HU代表平均CT值, SD代表噪声; 采用(HU—HUROI7)/SDROI7计算对比度噪声比(contrast-to-noise ratio, CNR), HUROI7代表脂肪的平均CT值, SDROI7代表脂肪的噪声; 采用[(SDa—SDb)/SDa]×100%计算降噪率, 即b算法相对a算法的降噪率[14]。

1.4.2　定性图像质量评价

由两名高年资医师采用完全盲法(对病例信息和重建方法不知情)进行分析。采用5级评分法对图像的整体噪声水平、金属伪影区显示情况、两手臂间腹部组织结构显示情况进行评估。具体评价标准见表1。两名医师可自己调整窗宽、窗位、层面, 如果评估过程中结果出现

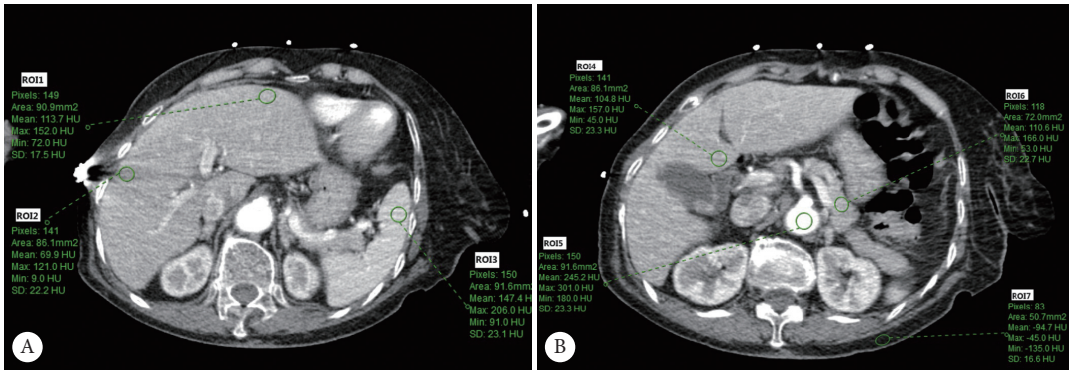

图 2　患者，女，70岁，CT腹部检查IR重建图像中ROI的设置

Fig 2　ROI setting in IR reconstructed image of the CT abdominal examination of a 70-year-old female patient

A is a one-layer 2.5 mm CT image of the patient's upper abdomen containing ROI 1, ROI 2, and ROI 3. B is a one-layer 2.5 mm CT image of the patient's upper abdomen containing ROI 4, ROI 5, ROI 6, and ROI 7.

表 1　图像质量评估分级表

Table 1　Grading scales for image quality evaluation

Image noise	Metal artifact	Display of structures between the two arms	Score
The noise is apparently and completely nondiagnostic	Artifacts too heavy for image recognition	Unable to display	1
Heavy blurring of anatomical details due to significant noise	Artifacts more than acceptable level	Vaguely displayed	2
The noise is noticeable but acceptable	Acceptable level of artifacts	Visible display with poor edges and contrast	3
The noise is observable	Artifacts less than acceptable level	Visible display with good edges and contrast	4
Almost no noise	No artifacts	Sharp edges and clear contrast	5

分歧,则由两名放射科医师经协商后达成共识。

1.5 统计学方法

使用SPSS 24.0软件进行统计分析。CT值、SD值、SNR和CNR等定量分析数据采用单因素方差检验,差异有统计学意义的ROI区均采用事后检验进行两两比较,并使用Bonferroni法校正检验水准,以控制多重比较中的Ⅰ型错误。图像的整体噪声水平、金属伪影区显示情况、两手臂间腹部组织结构显示情况等定性分析采用Kruskal–Wallis *H*检验。$P<0.05$为差异有统计学意义。

2 结果

2.1 患者特征

102例危重患者(67 例男性,35 例女性)的平均年龄为(54±12.3)岁,平均体质量指数为(23.23±3.51) kg/m^2,危重患者59例来自于ICU,43例来自于急诊创伤,平均容积CT剂量指数(volume CT dose index, CTDIvol)为(14.51±2.39) mGy。

2.2 定量分析结果

2.2.1 肝脏有金属伪影区域

DLMAR组与FBP组、IR组、DL组的CT值差异有统计学意义($P<0.01$);DLMAR组与FBPMAR组、IRMAR组的CT值差异无统计学意义;FBPMAR、IRMAR、DLMAR 3组间SD、SNR、CNR差异有统计学意义($P<0.01$),SD为DLMAR< IRMAR< FBPMAR,SNR和CNR均为DLMAR> IRMAR> FBPMAR。见表2。

2.2.2 两手臂间区域

6种重建方式CT值差异均无统计学意义。在ROI3、ROI4、ROI5:SD为DLMAR< DL< IRMAR< IR< FBPMAR<

表 2 定量分析图像质量的结果

Table 2 Results of quantitative analysis of image quality

Parameter		FBP	IR	DL	FBPMAR	IRMAR	DLMAR	*P*
ROI 1	Attenuation/HU	101.4±2.9	101.8±2.2	102.7±2.5	100.1±2.5	101.2±2.5	101.8±1.8	0.54
	SD/HU	19.8±1.8*	12.7±1.5*	10.5±1.2	19.3±1.6*	12.6±1.5*	10.7±1.3	<0.01
	CNR	10.2±0.9*	15.9±1.9*	19.3±2.3	10.4±0.9*	16.1±2.0*	18.9±2.4	<0.01
	SNR	5.2±0.5*	8.1±1.0*	9.9±1.2	5.2±0.5*	8.2±1.1*	9.6±1.3	<0.01
ROI 2	Attenuation/HU	73.7±5.6*	75.3±7.5*	66.3±11.4*	99.8±4.8	99.6±3.4	98.5±9.8	<0.01
	SD/HU	23.9±4.3*	14.9±2.2*	19.7±5.4*	19.3±3.1*	12.5±1.5*	11.1±1.3	<0.01
	CNR	7.4±1.4*	11.9±1.9*	9.1±3.1*	10.6±1.8*	16.0±2.1*	18.0±2.5	<0.01
	SNR	3.2±0.6*	5.2±0.9*	3.7±1.4*	5.3±0.9*	8.1±1.1*	9.0±1.5	<0.01
ROI 3	Attenuation/HU	136.0±2.9*	136.6±2.6	137.3±2.1	137.0±3.0	136.9±2.6	137.0±2.3	0.16
	SD/HU	27.8±1.8*	20.9±1.7*	17.1±1.7*	25.6±1.5*	19.6±1.7*	15.5±1.5	<0.01
	CNR	8.5±0.6*	11.3±1.0*	13.8±1.3*	9.3±0.6*	12.1±1.1*	15.4±1.4	<0.01
	SNR	4.9±0.4*	6.6±0.6*	8.1±0.8*	5.4±0.3*	7.1±0.7*	9.0±0.9	<0.01
ROI 4	Attenuation/HU	100.1±3.5	99.3±10.1	100.8±2.4	101.3±2.2	101.5±2.3	101.2±2.7	0.48
	SD/HU	27.0±1.9*	18.8±1.8*	14.1±1.7*	24.9±2.0*	16.8±1.8*	12.4±1.6	<0.01
	CNR	7.4±0.6*	10.6±1.2*	14.3±1.8*	8.1±0.7*	12.0±1.4*	16.4±2.1	<0.01
	SNR	3.7±0.3*	5.3±0.8*	7.2±0.9*	4.1±0.4*	6.1±0.7*	8.3±1.1	<0.01
ROI 5	Attenuation /HU	245.7±4.3	246.8±3.9	247.8±4.4	245.4±3.6	246.6±4.2	245.3±5.2	0.51
	SD/HU	25.2±2.1*	19.1±2.2*	14.2±1.6	24.1±1.9*	19.1±1.6*	13.9±1.7	<0.01
	CNR	13.7±1.2*	18.1±2.2*	24.7±2.8	14.4±1.1*	18.2±1.6*	25.1±3.3	<0.01
	SNR	9.8±0.8*	12.9±1.6*	17.7±2.0	10.3±0.8*	13.0±1.1*	17.9±2.4	<0.01
ROI 6	Attenuation/HU	117.1±2.3	116.6±2.0	115.6±2.4	118.4±2.7	117.3±2.3	115.7±2.1	0.37
	SD/HU	24.6±1.7*	16.3±1.4*	14.2±1.5*	20.2±1.8*	13.7±1.3*	12.5±1.4	<0.01
	CNR	8.8±0.6*	13.2±1.2*	15.2±1.6*	10.9±1.0*	15.9±1.6*	17.4±2.0	<0.01
	SNR	4.8±0.3*	7.1±0.7*	8.2±0.9*	5.9±0.6*	8.7±0.9*	9.4±1.1	<0.01

ROI: region of interest; HU: Hounsfield units; SNR: signal-to-noise ratio; CNR: contrast-to-noise ratio; FBP: filtered back projection; IR: iterative reconstruction; DL: deep learning reconstruction; FBPMAR: filtered back projection combined with smart metal artifact reduction; IRMAR: adaptive statistical iterative reconstruction-V combined with smart metal artifact reduction; DLMAR: deep learning reconstruction combined with smart metal artifact reduction. *P* value for one-way ANOVA intergroup differences.* $P<0.01$, vs. DLMAR group.

FBP, SNR和CNR均为DLMAR> DL> IRMAR> IR> FBPMAR> FBP; 在ROI6: SD为DLMAR< IRMAR< DL< IR< FBPMAR< FBP, SNR和CNR均为DLMAR> IRMAR> DL> IR> FBPMAR> FBP; 组间差异均有统计学意义(P< 0.01); 与FBP组相比, DLMAR的降噪率在ROI3、ROI4、ROI5、ROI6分别为44.2%、54.0%、44.8%、49.1%; 与IR组相比, DLMAR的降噪率在ROI3、ROI4、ROI5、ROI6分别为25.8%、34.0%、31.4%、23.3%; 与DL组相比, DLMAR的降噪率在ROI3、ROI4、ROI5、ROI6分别为9.3%、12.0%、2.1%、11.9%; 与FBPMAR组相比, DLMAR的降噪率在ROI3、ROI4、ROI5、ROI6分别为39.4%、50.2%、42.3%、38.1%; 与IRMAR组相比, DLMAR的降噪率在ROI3、ROI4、ROI5、ROI6分别为20.9%、26.1%、27.2%、8.7%; 组间差异均有统计学意义(P< 0.01)。见表2。

2.2.3　肝脏无金属伪影区域

在ROI1, 6种重建方式CT值差异均无统计学意义。加MAR前后两组间SD、SNR、CNR无明显差异(P> 0.05); SD为DLMAR/DL< IRMAR/IR< FBPMAR/FBP, SNR和CNR均为DLMAR/DL> IRMAR/IR> FBPMAR/FBP, 组间差异均有统计学意义(P< 0.01)。见表2。

2.3　定性分析结果

基于主观评估标准的平均得分如表3所示。加MAR的FBPMAR、IRMAR、DLMAR组在去金属伪影方面的得分均分别高于FBP、IR、DL组(P< 0.01)。DLMAR组在两手臂间结构显示得分4.62±0.37, 在图像降噪得分4.53±0.39, 均高于其他组(P< 0.01)。具体示例见图3。

表 3　图像质量定性评分结果

Table 3　Results of qualitative assessment of image quality

Image quality	FBP	IR	DL	FBPMAR	IRMAR	DLMAR	*P*
Metal artifact	1.36±0.54*	1.32±0.45*	1.24±0.46*	4.27±0.32*	4.44±0.34*	4.61±0.28	<0.01
Display of structures between the two arms	3.33±0.71*	3.94±0.58*	4.52±0.65*	3.41±0.55*	4.23±0.47*	4.62±0.37	<0.01
Image noise	3.24±0.57*	3.66±0.53*	4.36±0.37*	3.27±0.61*	4.25±0.41*	4.53±0.39	<0.01

The abbreviations are explained in the note to Table 2.

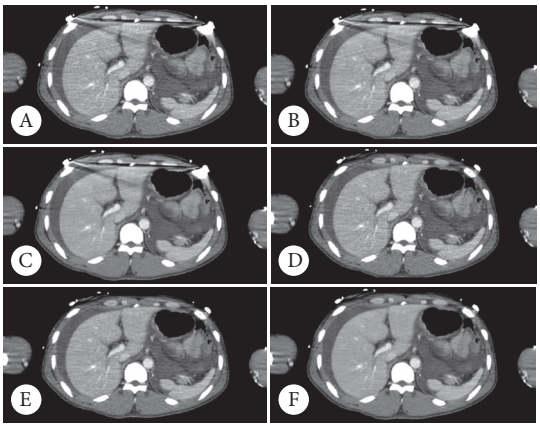

图 3　患者上腹部CT静脉期图像（男，79岁，重物砸伤，昏迷）

Fig 3　Upper abdominal CT image of the venous phase (a 79-year-old comatose male patient struck and injured by a heavy object)

A, FBP; B, IR; C, DL; D, FBPMAR; E, IRMAR; F, DLMAR. Compared to the other reconstructions, the DLMAR image has better clarity, less noise, less streaks of artifacts due to lateral arms, and less metal artifacts.

3　讨论

本研究的目的是评估DLMAR技术重建的应用是否可以提高危重患者上腹部CT成像的图像质量。结果表明, FBP、IR、DL、FBPMAR、IRMAR、DLMAR重建的CT图像的客观图像质量参数存在明显差异, 主观评价也存在差异。其中与其他重建相比, DLMAR可以减少金属伪影和手臂间条纹伪影, 降低噪声, 提高SNR, 提升图像质量。

改变手臂位置被认为是减少手臂伪影最有用和最方便的方法之一[15]。KAHN等[16]和FLEISCHMANN等[17]评估了不同手臂位置对腹部图像质量的影响, 并证明举起至少一只手臂或将手臂放在上腹部前方而不是躯干旁边可以提高图像质量。但这取决于患者的病情, 对于本研究的对象较难实现。IR 算法提供在低辐射剂量数据集中降低噪声的能力, 目前最新IR重建算法如ASiR-V等基于模型的IR, 使用几何和统计模型(如焦点、体素和探测器尺寸)利用物理模型和医学图像的特征来校正图像的初始计算值[18]。本研究结果中, IR相比FBP在两手臂间组织显示更清楚, 噪声更低, 有更高的SNR与CNR, 这与之前的研究一致[18-19]。

基于人工智能框架的图像质量优化技术已备受关注。凭借创新的设计和先进的训练方法, 可实现智能图像降噪并恢复首选噪声纹理, 与FBP、IR相比, 可提高客观和主观图像质量[20-21]。JENSEN等[22]研究评估了DL重建的图像质量, 将其与临床常用的FBP和IR进行比较, 表明DL在腹部的图像噪声和清晰度方面优于IR[22]。PARK等[23]表明, DL重建在下肢CT血管造影的图像噪声和清晰度方面优于ASiR-V。JENSEN等[24]的研究对高强度DL图

像中小病变和血管可能模糊表示担忧，因此本研究选择中等强度重建。本研究结果显示 DL重建相比FBP、IR在两手臂间组织的显示更清楚，SNR与CNR更高，噪声更低。FUJITA等[25]研究也有相似结果，表明DL重建相比于IR、FBP，可以减少两手臂间腹部组织的条纹伪影。

对于本研究的对象，不仅两手臂间会产生横向的条纹伪影、增加噪声，心电监护的电极与电极线还会产生金属伪影。当 X射线束穿过监护电极及线等金属时，因为金属物体具有高衰减系数，X射线会明显衰减，且到达探测器元件的光子太少。这种光子饥饿导致探测器产生不足的信号，并导致重建过程中的零透射投影和不正确的计算[6]。IR、DL都不能很好解决金属伪影[26-27]。研究表明Smart MAR技术算法对图像质量客观参数有改善[28]。该技术可以有效地揭示隐藏在金属附近的伪影下方的解剖细节，可减少骨科植入物患者的金属伪影[29-30]。本研究定性结果表明，加MAR的FBPMAR、IRMAR、DLMAR相比FBP、IR、DL可减少金属伪影，DLMAR组去金属伪影、两手臂间组织结构显示、图像噪声的主观评分均明显高于其他组。定量分析与这一结果相印证，DLMAR可纠正在肝脏金属伪影区域CT值；相比其他组，可提高在两手臂间组织的SNR与CNR，降低噪声。定量结果表明在两手臂间组织加MAR可以降低噪声，提高图像质量。但在肝脏无金属伪影区域，加MAR对图像质量没有影响。DLMAR结合人工智能技术与MAR算法去金属伪影的优点，使得DLMAR能够有效减少图像的噪声、条纹伪影以及金属伪影，改善手臂不能上举且有心电监护的电极与电极线的上腹部图像质量。

本研究的局限性：①虽然良好的图像质量是诊断的基础，但本研究只探讨了两手臂之间以及金属伪影区域的解剖结构显示的情况，并没有评估伪影对病灶显示及疾病诊断的影响，这将在随后的研究中涉及。②心电监护的电极、电极线以及手臂的位置不固定，故ROI测量解剖层面每例患者有一定差异，这可能会使结果产生偏差。③DL以及IR重建算法的权重参数只选择一种，没有进行多重建权重的比较，将在未来的研究中进一步探索。

总之，在双手臂不能上举且需要心电监护的危重患者中，DLMAR可以减少伪影、降低噪声，提升上腹部CT图像质量，为临床医生提供准确、可靠的信息，有助于更好地诊断和治疗危重患者。

* * *

作者贡献声明 潘云龙负责论文构思、正式分析、研究方法、软件、初稿写作和审读与编辑写作，姚小玲负责调查研究、研究项目管理、监督指导和审读与编辑写作，高荣慧负责调查研究、软件和验证，谢薇负责调查研究、验证和可视化，夏春潮负责研究项目管理、提供资源和监督指导，李真林负责经费获取、提供资源、监督指导和审读与编辑写作，孙怀强负责论文构思、数据审编、提供资源、监督指导、验证和审读与编辑写作。所有作者已经同意将文章提交给本刊，且对将要发表的版本进行最终定稿，并同意对工作的所有方面负责。

Author Contribution PAN Yunlong is responsible for conceptualization, formal analysis, methodology, software, writing--original draft, and writing--review and editing. YAO Xiaoling is responsible for investigation, project administration, supervision, and writing--review and editing. GAO Ronghui is responsible for investigation, software, and validation. XIE Wei is responsible for investigation, validation, and visualization. XIA Chunchao is responsible for project administration, resources, and supervision. LI Zhenlin is responsible for funding acquisition, resources, supervision, and writing--review and editing. SUN Huaiqiang is responsible for conceptualization, data curation, resources, supervision, validation, and writing--review and editing. All authors consented to the submission of the article to the Journal. All authors approved the final version to be published and agreed to take responsibility for all aspects of the work.

利益冲突 所有作者均声明不存在利益冲突

Declaration of Conflicting Interests All authors declare no competing interests.

参 考 文 献

[1] ACQUISTO N M, MOSIER J M, BITTNER E A, *et al*. Society of Critical Care Medicine Clinical Practice Guidelines for rapid sequence intubation in the critically ill adult patient. Crit Care Med, 2023, 51(10): 1411-1430. doi: 10.1097/ccm.0000000000006000.

[2] LANSIER A, BOURILLON C, CUÉNOD C A, *et al*. CT-based diagnostic algorithm to identify bowel and/or mesenteric injury in patients with blunt abdominal trauma. Eur Radiol, 2023, 33(3): 1918-1927. doi: 10.1007/s00330-022-09200-9.

[3] FATHI M, MIRJAFARI A, YAGHOOBPOOR S, *et al*. Diagnostic utility of whole-body computed tomography/pan-scan in trauma: a systematic review and meta-analysis study. Emerg Radiol, 2024, 31(2): 251-268. doi: 10.1007/s10140-024-02213-5.

[4] ACHATZ G, SCHWABE K, BRILL S, *et al*. Diagnostic options for blunt abdominal trauma. Eur J Trauma Emerg Surg, 2022, 48(5): 3575-3589. doi: 10.1007/s00068-020-01405-1.

[5] BENNEKER L M, BONEL H, ZUMSTEIN M, *et al*. A novel multiple-trauma CT-scanning protocol using patient repositioning may increase risks of iatrogenic injuries. Emerg Radiol, 2007, 13: 349-351. doi: 10.1007/s10140-007-0577-1.

[6] SELLES M, Van OSCH J A C, MAAS M, *et al*. Advances in metal artifact reduction in CT images: A review of traditional and novel metal artifact reduction techniques. Eur J Radiol, 2024, 170: 111276. doi: 10.1016/j.ejrad.2023.111276.

[7] HODGETTS T J, KENWARD G, VLACHONIKOLIS I G, *et al*. The identification of risk factors for cardiac arrest and formulation of activation criteria to alert a medical emergency team. Resuscitation, 2002, 54(2): 125-131. doi: 10.1016/s0300-9572(02)00100-4.

[8] YASAKA K, FURUTA T, KUBO T, *et al*. Full and hybrid iterative reconstruction to reduce artifacts in abdominal CT for patients scanned

without arm elevation. Acta Radiol, 2017, 58(9): 1085-1093. doi: 10.1177/0284185116684675.

[9] KATARIA B, NILSSON ALTHÉN J, SMEDBY Ö, *et al*. Image quality and potential dose reduction using advanced modeled iterative reconstruction (admire) in abdominal CT--a review. Radiat Prot Dosimetry, 2021, 195(3/4): 177-187. doi: 10.1093/rpd/ncab020.

[10] MILETO A, GUIMARAES L S, MCCOLLOUGH C H, *et al*. State of the art in abdominal CT: the limits of iterative reconstruction algorithms. Radiology, 2019, 293(3): 491-503. doi: 10.1148/radiol.2019191422.

[11] MüCK J, REITER E, KLINGERT W, *et al*. Towards safer imaging: A comparative study of deep learning-based denoising and iterative reconstruction in intraindividual low-dose CT scans using an in-vivo large animal model. Eur J Radiol, 2024, 171: 111267. doi: 10.1016/j.ejrad.2023.111267.

[12] 曾令明, 徐旭, 曾文, 等. 基于深度学习的重建算法在健康志愿者肝脏低剂量薄层CT检查中的应用研究. 四川大学学报(医学版), 2021, 52(5): 807-812. doi: 10.12182/20210660103.
ZENG L M, XU X, ZENG W, *et al*. Application of deep learning reconstruction algorithm in low-dose thin-slice liver CT of healthy volunteers. J Sichuan Univ (Med Sci), 2021, 52(5): 807-812. doi: 10.12182/20210660103.

[13] BRANCO D, KRY S, TAYLOR P, *et al*. Evaluation of image quality of a novel computed tomography metal artifact management technique on an anthropomorphic head and neck phantom. Phys Imaging Radiat Oncol, 2021, 17: 111-116. doi: 10.1016/j.phro.2021.01.007.

[14] OOSTVEEN L J, SMIT E J, DEKKER H M, *et al*. Abdominopelvic CT image quality: evaluation of thin (0. 5-mm) slices using deep learning reconstruction. AJR Am J Roentgenol, 2023, 220(3): 381-388. doi: 10.2214/AJR.22.28319.

[15] BAYER J, PACHE G, STROHM P C, *et al*. Influence of arm positioning on radiation dose for whole body computed tomography in trauma patients. J Trauma, 2011, 70(4): 900-905. doi: 10.1097/TA.0b013e3181edc80e.

[16] KAHN J, GRUPP U, MAURER M. How does arm positioning of polytraumatized patients in the initial computed tomography (CT) affect image quality and diagnostic accuracy? Eur J Radiol, 2014, 83(1): e67-e71. doi: 10.1016/j.ejrad.2013.10.002.

[17] FLEISCHMANN D, EDWARD BOAS F. Computed tomography--old ideas and new technology. Eur Radiol, 2011, 21(3): 510-517. doi: 10.1007/s00330-011-2056-z.

[18] UNGANIA S, SOLIVETTI F M, D'ARIENZO M, *et al*. New-generation ASiR-V for dose reduction while maintaining image quality in CT: a phantom study. Applied Sciences, 2023, 13(9): 5639-5650. doi: 10.3390/app13095639.

[19] KAWASHIMA H, ICHIKAWA K, TAKATA T, *et al*. Algorithm-based artifact reduction in patients with arms-down positioning in computed tomography. Phys Med, 2020, 69: 61-69. doi: 10.1016/j.ejmp.2019.11.019.

[20] SOLOMON J, LYU P, MARIN D, *et al*. Noise and spatial resolution properties of a commercially available deep learning-based CT reconstruction algorithm. Med Phys, 2020, 47(9): 3961-3971. doi: 10.1002/mp.14319.

[21] SZCZYKUTOWICZ T P, NETT B, CHERKEZYAN L, *et al*. Protocol optimization considerations for implementing deep learning CT reconstruction. AJR Am J Roentgenol, 2021, 216(6): 1668-1677. doi: 10.2214/AJR.20.23397.

[22] JENSEN C T, GUPTA S, SALEH M M, *et al*. Reduced-dose deep learning reconstruction for abdominal CT of liver metastases. Radiology, 2022, 303(1): 90-98. doi: 10.1148/radiol.211838.

[23] PARK C, CHOO K S, JUNG Y, *et al*. CT iterative vs deep learning reconstruction: comparison of noise and sharpness. Eur Radiol, 2021, 31(5): 3156-3164. doi: 10.1007/s00330-020-07358-8.

[24] JENSEN C T, LIU X, TAMM E P, *et al*. Image quality assessment of abdominal CT by use of new deep learning image reconstruction: initial experience. AJR Am J Roentgenol, 2020, 215(1): 50-57. doi: 10.2214/AJR.19.22332.

[25] FUJITA N, YASAKA K, KATAYAMA A, *et al*. Assessing the effects of deep learning reconstruction on abdominal CT without arm elevation. Can Assoc Radiol J, 2023, 74(4): 688-694. doi: 10.1177/08465371231169672.

[26] OOSTVEEN L J, MEIJER F J, De LANGE F, *et al*. Deep learning–based reconstruction may improve non-contrast cerebral CT imaging compared to other current reconstruction algorithms. Eur Radiol, 2021, 31(8): 5498-5506. doi: 10.1007/s00330-020-07668-x.

[27] KOETZIER L R, MASTRODICASA D, SZCZYKUTOWICZ T P, *et al*. Deep learning image reconstruction for CT: technical principles and clinical prospects. Radiology, 2023, 306(3): e221257. doi: 10.1148/radiol.221257.

[28] PUVANASUNTHARARAJAH S, FONTANAROSA D, WILLE M L, *et al*. The application of metal artifact reduction methods on computed tomography scans for radiotherapy applications: a literature review. J Appl Clin Med Phys, 2021, 22(6): 198-223. doi: 10.1002/acm2.13255.

[29] 杨帆, 梁译文, 邵强, 等. MAC技术在全髋关节置换术后CT去金属伪影中的应用. 四川大学学报(医学版), 2020, 51(6): 828-833. doi: 10.12182/20201160603.
YANG F, LIANG Y W, SHAO Q, *et al*. Application value of CT metal artifact correction technology (MACTM) in CT review after total hip replacement. J Sichuan Univ (Med Sci), 2020, 51(6): 828-833. doi: 10.12182/20201160603.

[30] FELDHAUS F W, BÖNING G, KAHN J, *et al*. Improvement of image quality and diagnostic confidence using Smart MAR--a projection-based CT protocol in patients with orthopedic metallic implants in hip, spine, and shoulder. Acta Radiol, 2020, 61(10): 1421-1430. doi: 10.1177/0284185120903446.

（2024 – 05 – 14收稿, 2024 – 11 – 09修回）

编辑　余　琳